Effect of aging time on the sustainability of microstructure, corrosion, and mechanical of Al6061

Akinsanya Damilare Baruwa[1*] and *Mamookho* Elizabeth Makhatha[1]

[1]Metallurgy Department, University of Johannesburg, Johannesburg, South Africa.

Abstract. The high corrosion resistance of Al 6061 has made the material for wide applications. However, for its sustainability in applications, the mechanical properties and corrosion resistance have to be improved through modifications such as heat treatment. Therefore, the study investigates the influence of the aging time on the corrosion resistance, mechanical properties, and microstructure of the material after heat treatment. Al 6061 will be investigated at T0, T4, and T6- for 30 mins, 60 mins and 90 mins using water as the cooling media. The microstructure was observed using light microscope, the corrosion rate was determined by potentiostat using seawater as the electrolyte, and hardness was measured through Brinell's scale and the tensile test machine to investigate its UTS and elongation. It was discovered that the samples quenched before aging had improved properties compared to the samples that were normalized. The colling method shows a greater impact on the properties of the material.

1 Introduction

Aluminum 6061 (Al6061) is a widely used alloy in various industries, known for its exceptional combination of strength to weight ratio, formability, and corrosion resistance [1–3]. This makes it applicable to a wide range of applications, including aerospace, marine, biomedical,nd automobile [3,4]. However, applications nowadays require further treatments to improve its properties, including structures.

Al6061 has different microstructures, depending on the type of heat treatment conducted on the as-cast [5]. The Microstructure of Al6061 evolves over time due to a process called aging, which involves the controlled precipitation of strengthening phases [6]. Aging plays a pivotal role in tailoring the material's mechanical properties, as well as its resistance to corrosion [7].

Understanding the effect of aging time on the microstructure and subsequent material properties is of great significance for optimizing the performance and reliability of metals such as Al6061 in practical applications. Solid solution diffusion and coherent precipitates could be formed in the matrix during the aging process due to solute atoms in the supersaturated condition [8]. Therefore, distribution, density, and sizes of these precipitates

* Corresponding authors: darebaruwa@gmail.com

significantly influence the material's yield strength, tensile strength, and hardness properties[9]. It is also evident in previous studies that aging influences the corrosion behavior of any alloy [10]. The alloy's susceptibility can be altered during aging because of specific precipitation to form corrosive environments that may lead to localized corrosion, affecting the material's overall integrity [11].

For this reason, this investigation aims to study the impact of aging time on the microstructure, corrosion resistance, and necessary mechanical properties of Al6061. Understanding the kinetics of precipitation and the development of strengthening phases during aging will give insights into the material's performance over time. This could be achieved by controlling the aging parameters, to tailor the microstructure, mechanical and corrosion properties of the material to meet specific engineering requirements. Overall, the findings will promote an in-depth knowledge of the impact of aging time on the microstructure, corrosion resistance, and mechanical properties of Al6061. This will facilitate the engineering design of Al6061 alloys with enhanced performance and extended service life in critical applications across industries.

2 Methodology

The as-cast Al6061 was supplied by Metal Centre, South Africa, which had chemical composition of Si (1.87), Fe (0.40), Mg (1.13), Cu (0.38), Ag (1.09) and Al- the balance as determined from the spark spectrometer.
The specimens were subjected to heat treatments by considering two distinct techniques: natural heat treatment and artificial heat treatment. For the natural method (T4), the samples were subjected to a heating temperature of 610°C for a duration of 5 hours, and then quenched to room temperature in water. On the other hand, for the artificial treatment (T6), it involved heating the samples to 610°C for 5 hours, and subsequently quenching them to room temperature in water. The specimens were further placed inside an oven and subjected to an aging process at 200°C for three different time intervals: 30 minutes, 60 minutes, and 90 minutes (1h: 30m).
To investigate the effects of heat treatments on the samples, detailed experimental analyses were conducted. Optical microscopy was used to characterize the microstructural features, grain size, and precipitate distribution. Corrosion resistan ce was measured through 3-electrode cell (SCE, Al6061, and platinum) electrochemical tests adopting potentiodynamic polarization method in a NaCl environment. Furthermore, tensile tests, and hardness measurements were performed to assess the mechanical properties of the samples.

3 Results and Discussion

3.1 Microstructure

Fig. 1 illustrates the optical microscope microstructure of Al6061 samples in their as-received state, as well as after undergoing T4, T6 treatment for 30 minutes, T6 treatment for 1 hour, and T6 treatment for 1 hour and 30 minutes, respectively. The seawater was fetched from Indian ocean at Durban beach front.

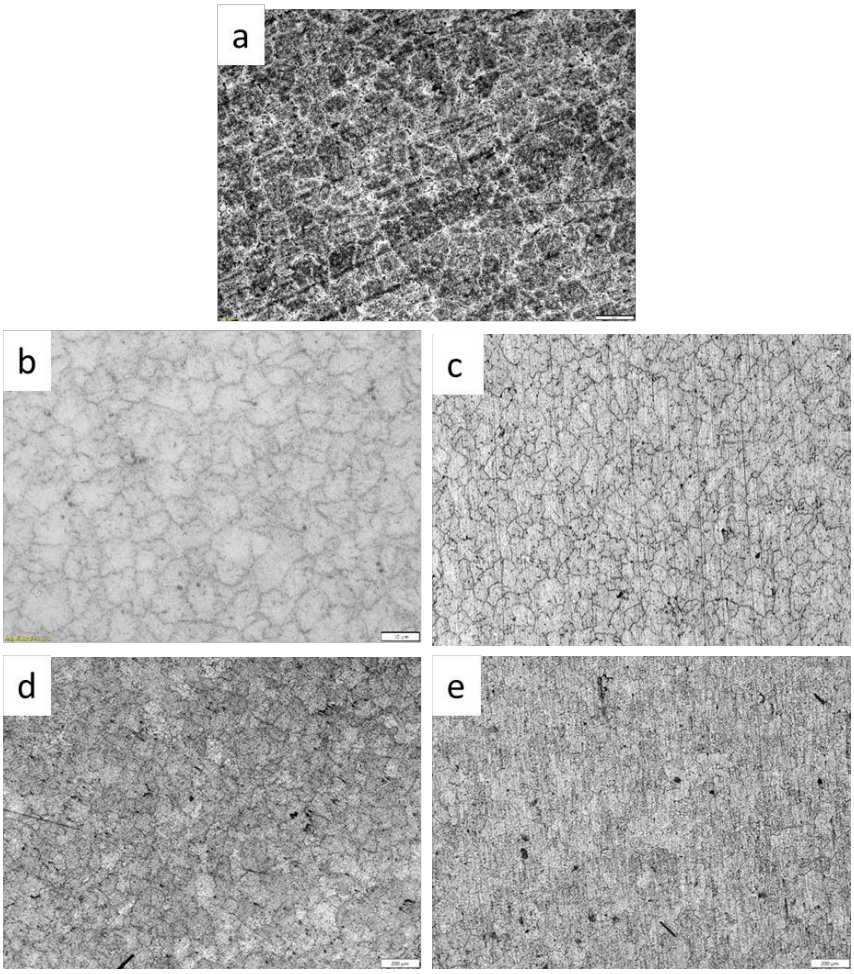

Fig. 1: The microstructure of the a) as-cast, b) T4, c) T6 30 minutes, d) T6 1 hour and e) 1 hour 30 minutes

In its as-received condition (Fig. 1a), the sample displays larger grain structures with fewer grain boundaries. Notably, clusters of magnesium (Mg) and silicon (Si) particles do not form as the material solidifies. These characteristics contribute to the material's inherent ductility. Consequently, the mechanical properties such as hardness, toughness, and strength are expected to be relatively low. This could be due to the increased mobility of dislocations within the alloy during deformation, owing to the aforementioned microstructural attributes. Fig. 1b depicts the microstructural characteristics of the T4 sample. The T4 sample exhibits a moderate grain size, which is notably smaller than that of the as-received sample. This reduction in grain size is accompanied by a decrease in the abundance of grain boundaries, although they still remain less prevalent than in the original as-received state. Notably, clusters composed of magnesium (Mg) and silicon (Si) (the EDS not shown) with a medium particle size have emerged, primarily situated around grain boundaries. However, it's important to note that these clusters are not uniformly distributed throughout the microstructure. Microstructures of this nature typically result in mechanical properties of a moderate nature. This arises from the inherent difficulty that dislocations encounter when attempting to traverse freely through a single crystal lattice. As a result, the material's behaviour under load is characterized by a balance between strength and ductility, making it

suitable for applications that demand a combination of both attributes [12]. In Fig. 1c, represents the microstructure of the T6-30 mins sample. This microstructure is characterized by an abundance of exceptionally small grains. Within this structure, clusters of magnesium (Mg) and silicon (Si) have formed, and remarkably, these clusters are well-distributed across the sample's surface. This microstructural configuration is conducive to the development of favourable mechanical properties, encompassing attributes such as heightened hardness and strength. The densely packed grain boundaries and the associated obstacles for dislocation movement contribute to the overall robustness of the material, rendering it well-suited for applications demanding resilience under stress and load. Displayed in Figs. 1d and 1e are the microstructures of T6 samples subjected to treatments lasting 1 hour and 1 hour and 30 minutes, respectively. The microstructural configuration evident in both Figures corresponds to what is commonly referred to as "peak-aged" microstructure. This nomenclature is rooted in the prevalence of numerous clusters composed of minuscule particles, specifically Mg_2Si. Remarkably, these microstructures exhibit grain sizes of such diminutive scale that they remain imperceptible when viewed under a 50 µm magnification. This observation is indicative of a profusion of grains within the material. This structural characteristic, in turn, engenders exceptional mechanical properties, remarkably a pronounced elevation in hardness and strength. The abundance of finely distributed grain boundaries effectively impedes the mobility of dislocations, underscoring the material's capacity to excel in applications requiring substantial resistance against external forces and exceptional load-bearing capabilities [13]. Due to the use of artificial aging, fine precipitates are formed not only at grain boundaries, but also randomly distributed in free positions in the crystal lattice of all grains. This greatly improves the mechanical properties and, when sufficiently aged, improves corrosion resistance by preventing the tendency for localized intergranular corrosion. Artificial aging time is inversely proportional to temperature and can vary greatly from alloy to alloy, even with multi-stage treatments. The high-temperature treatment at the beginning of the production phase determines the size, shape, and distribution of intermetallic particles, which trap the dislocations and serve as nucleation sites for precipitates.

3.2 Hardness

Hardness stands as a pivotal attribute intricately linked to a material's adaptable and malleable characteristics. This testing method, often straightforward in execution, yields outcomes that can be correlated with a spectrum of other mechanical traits encompassing tensile strength, toughness, ductility, and more. Within the scope of this project, Brinell's hardness testing was conducted, yielding outcomes that are presented in Fig. 2.

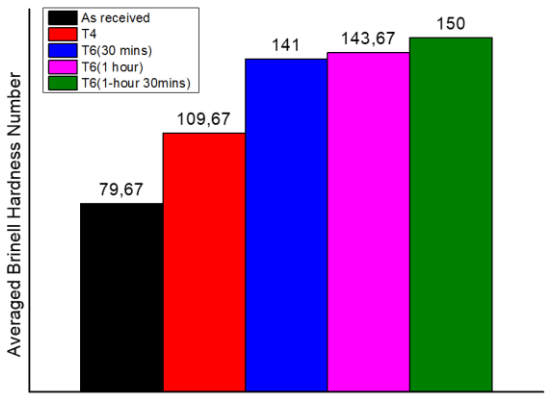

Fig. 2: The averaged hardness of the as-cast and the heat-treated samples

The data shows the evolution of hardness after subjection to different heat treatments. From the data, the hardness of the material improves as the aging time increases. Before heat treatment, the samples were held at room temperature for a week to facilitate the improvement of the mechanical properties of the AA6061-T6, which also impacts its hardness value. This shows the influence of a specific aging period on the material's performance and good properties. Also, the improvement of the material over aging time can be attributed to the compactness of the microstructure and the immobility of structural grains due to refinements [14].

3.3Tensile

Fig. 3 presents an overview of the ultimate tensile strengths (UTS) and elongation values derived from the conducted tensile tests. The results are indicative of the mechanical behaviour exhibited by the samples treated at various conditions.

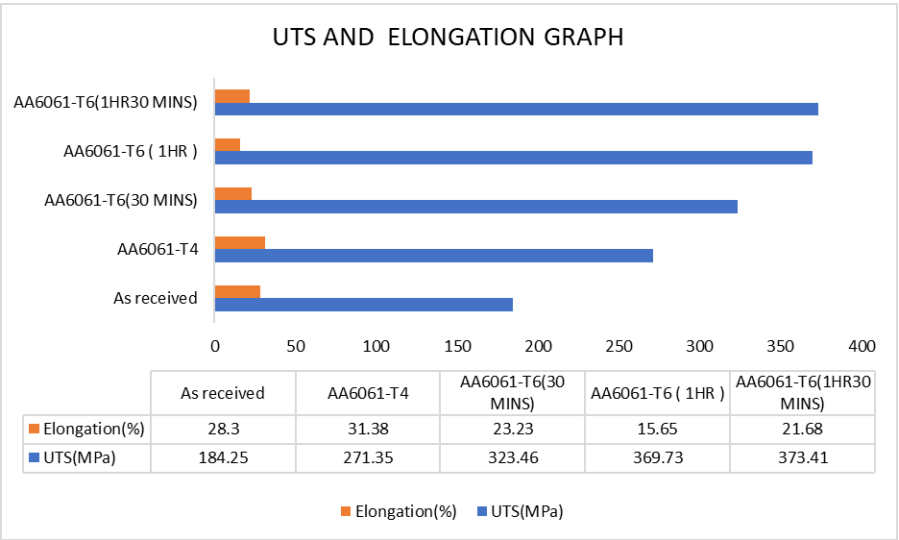

	As received	AA6061-T4	AA6061-T6(30 MINS)	AA6061-T6 (1HR)	AA6061-T6(1HR30 MINS)
Elongation(%)	28.3	31.38	23.23	15.65	21.68
UTS(MPa)	184.25	271.35	323.46	369.73	373.41

Fig. 3: Averaged tensile strength of the ass-cast and heat-treated samples

Specifically, the UTS values recorded for these samples are as follows: 184.245 MPa for the as-received sample, 271.345 MPa for the natural (T4) state, 323.459 MPa following T6 treatment for 30 minutes, 369.729 MPa after T6 treatment for 1 hour, and 373.414 MPa subsequent to T6 treatment for 1 hour and 30 minutes. Correspondingly, the elongations for the respective specimens are 28.3%, 31.375%, 23.225%, 15.65%, and 21.675%, aligning with the same sequence as the UTS values. These data unveil a discernible trend, wherein the UTS consistently increases as the treatment time progresses, resulting in a corresponding decrease in elongation. This pattern underscores the impact of microstructural alterations on the mechanical properties of the materials, as longer treatment times correlate with enhanced strength but reduced ductility. The ultimate tensile strength across all samples exhibits improvement, albeit with a noticeable reduction in elongation among the T6 specimens when compared to the as-received sample. This decline in elongation is primarily attributed to the attainment of higher levels of hardness [15], a characteristic that is visually corroborated by the hardness bar graph and the stress-strain curve. In the samples investigated, it is pertinent

to state that only T4 sample retains the favourable properties that make it suitable for applications where a high risk of fracture could be prevalent. This could be attributed to the unique behaviour of T4, which demonstrates the highest elongation before fracture.
Precipitation stands as a widely adopted strategy aimed at enhancing the toughness of alloys characterized by structures encompassing finely dispersed particles that impede the movement of dislocations within a pliable matrix [16]. Notably, the degree of particle dispersion plays a pivotal role; the finer the distribution of particles with a consistent count, the more pronounced the material's strength becomes. This phenomenon finds validation through the observed hardness and strength values evident across all T6 samples. However, an extended aging period can potentially induce a transformation in the material's behaviour from ductile to brittle, as vividly determined from the elongation percentage. A direct consequence of this transformation is the reduction in elongation for aged specimens. This shift towards heightened strength can inadvertently lead to a propensity for abrupt fracture without preceding indications [17]. This transformation towards brittleness significantly restricts the potential applications of the alloy. For instance, in shipbuilding, such a brittle material would not be deemed suitable for hull construction, as it could succumb to fractures upon collision with solid objects within the cold seawater environment.

3.4 Corrosion

The effect of aging time on the corrosion resistance of the heat-treated materials was investigated using the linear polarization method by monitoring both anodic and cathodic curves, and the curves and emanating data is presented in Fig. 4 and Table 1.

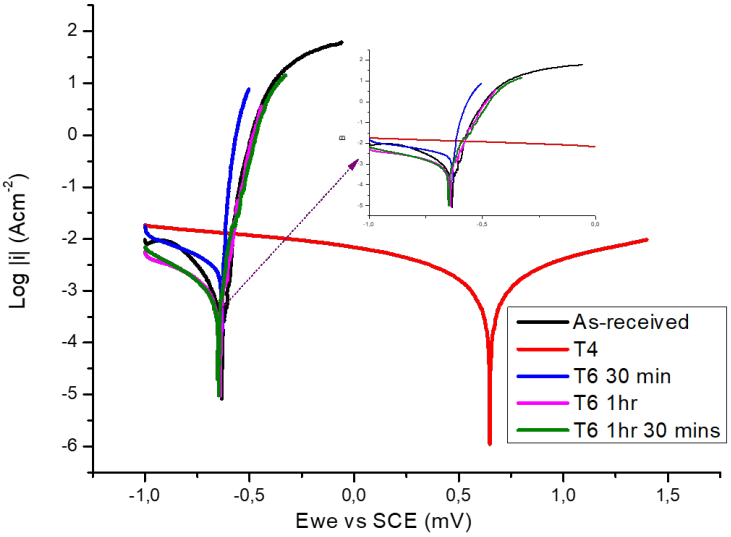

Fig. 4: The polarization curve of heat-treated samples

From Fig. 4 and Table 1, it is clear that the lower corrosion current permissibility increases as the aging time increases. This corroborates the effect of the microstructural grains and structures on the ability to resist corrosion. The finer the grains, the more compact the microstructure, and the lower the permeability of the electrolyte into the structure. Although the corrosion potential of both the as-received and the aged samples are almost equal, the corrosion current densities, however, reduced over time. The effect of the aging time is also observed in the corrosion rate and efficiency. The higher the aging time, the lower the

corrosion rate and the higher the efficiency of the Al6061 to resist corrosion in natural seawater. The corrosion efficiency n_p was calculated using the method in Eq. 1.

$$n_p\% = \frac{I_{corr}+I^{i}_{corr}}{I_{corr}} \quad (1)$$

Where I_{corr} is the corrosion density of the as-received while I^{i}_{corr} is the corrosion density for the heat-treated samples.

Table 1: The corrosion parameters obtained from the fitting of the Tafel plot

Samples	**As-received**	**T4**	**T6 30 mins**	**T6 1 hr**	**T6 1hr 30 min**
E_{corr} (mV)	-642.642	885.434	-649.379	-649.379	-647.434
I_{corr} (μA)	4.909	3.232	1.408	1.323	0.805
β_c (mV)	1 156.2	2 499.0	337.3	630.7	380.7
β_a (mV)	67.9	296.5	077.3	059.0	057.6
R (mΩ)	130.911	273.959	461.207	490.838	804.266
Corrosion rate (mmpy)	0.0749572	0.0493505	0.0214992	0.0202013	0.0122918
% Efficiency		34.2	71.3	73.0	83.6

The enhancement of corrosion resistance in the aged Al6061 may be attributed to the presence of oxides originating from the precipitates that formed MgO and SiO_2 on the surface of the materials after aging. During the investigation of the microstructure, it was observed that the higher the aging time, the more precipitate was produced. Hence, denser oxides will be formed on the longer-aged samples and, thereby improving the corrosion resistance [18]. Also, the finer the microstructure of a material, the better the corrosion resistance of the material [19].

Moreover, the examination of the microstructure subsequent to the corrosion test was carried out using a scanning electron microscope. The resulting micrographs are depicted in Figs. 5a-f. Specifically, Fig. 5a illustrates the surface characteristics of the Al6061 alloy as it was received, prior to subjecting it to the corrosion test. The surface appeared smooth, flat and without any deformation. Interestingly, the as-received Al6061 alloy (Fig. 5b) exhibited the most pronounced susceptibility to pitting corrosion when exposed to seawater among all the specimens investigated. This susceptibility is attributed to the absence of a protective oxide layer (Al_2O_3) on its surface. This is a notable observation, highlighting the lack of inherent corrosion protection in this state. Conversely, all the specimens treated under the T6 condition demonstrated notable resistance to pitting corrosion, a phenomenon attributed to the presence of chlorine ions in the seawater. Figs. 5d, e and f show a little dilapidation of the surface protection film that emanated from alumina oxide. This corroborates the results obtained from potentiodynamic polarization, whereby the T6 treatments resist corrosion propagation better than T4 treatment. Notably, the T4-treated specimen displayed an elevated localized corrosion rate when compared to the T6 treatments. This manifestation was visually evident through the formation of blisters and craters on the surface of the T4 specimen. These observations support the findings of other researchers [20].

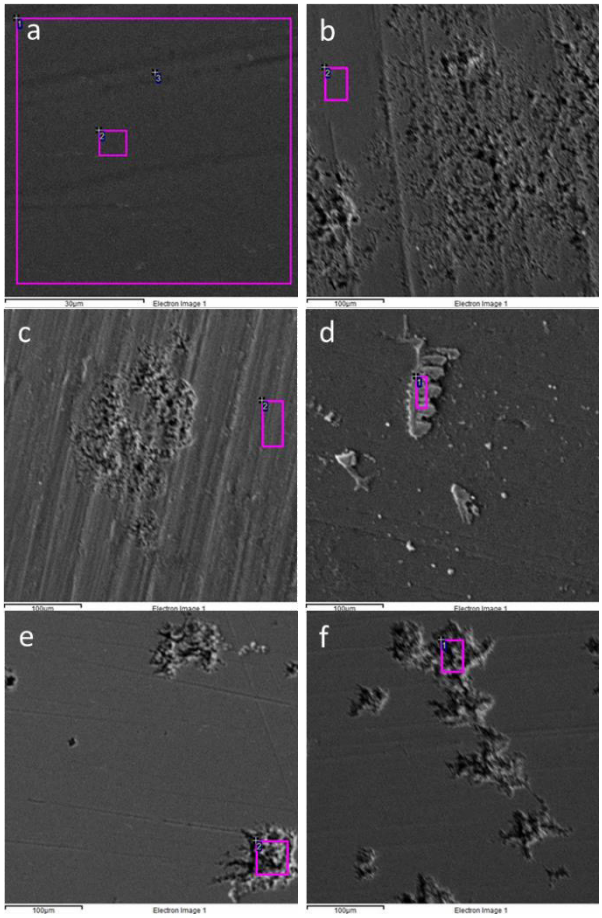

Fig. 5: The micrograph of the surface of a) as-cast before corrosion, b), as-cast c) T4, d) T6 30 minutes, e) T6 1 hour and f) 1 hour 30 minutes after corrosion

4 Conclusions

This study aims to explore how aging duration affects Al6061's microstructure, corrosion resistance, and mechanical properties for its sustainability during applications. By delving into the kinetics of precipitation and the development of strengthening phases during aging, valuable insights can be gleaned into the material's performance over time. The ability to manipulate aging parameters offers the prospect of tailoring microstructure and, consequently, mechanical and corrosion properties to fulfill specific engineering prerequisites.

Microstructural examination revealed distinct changes across various treatments. The as-received sample exhibited larger grains with fewer grain boundaries, while T4 showcased a moderate grain size reduction and emerging clusters of magnesium and silicon particles. The T6-30 mins sample displayed abundant small grains with well-distributed magnesium-silicon clusters, contributing to enhanced hardness and strength. For T6 samples treated longer, microstructures exhibited numerous clusters of minuscule particles, resulting in exceptional mechanical properties.

Hardness testing indicated a clear progression of hardness as treatment severity increased, indicating the influence of microstructural alterations. The ultimate tensile strength increased as treatment time progressed, along with a corresponding reduction in elongation, underscoring the relationship between microstructure, strength, and ductility.
Corrosion resistance improved with increased aging time due to the formation of oxide layers on the surface. The finer microstructure resulting from longer aging times led to denser oxides, enhancing resistance. The T4-treated specimen displayed the highest localized corrosion rate, while the T6-treated specimens showcased remarkable resistance attributed to the presence of chlorine ions in seawater.
In conclusion, this study unravelled the intricate connections between aging time, microstructure, corrosion resistance, and mechanical properties of Al6061. Such insights hold immense promise for optimizing Al6061 alloy performance for diverse and critical applications in various industries.

References

1. H. A. Almashhadani, M. K. Alshujery, M. Khalil, M. M. Kadhem, and A. A. Khadom, J Mol Liq **343**, (2021)
2. R. Maurya, B. Kumar, S. Ariharan, J. Ramkumar, and K. Balani, Mater Des **98**, 155 (2016)
3. V. Shrivastava, G. K. Gupta, and I. B. Singh, J Alloys Compd **775**, 628 (2019)
4. V. K. Sharma, V. Kumar, and R. S. Joshi, Journal of Materials Research and Technology **8**, 3504 (2019)
5. N. Liu, L. Ma, A. J. Liu, Z. Zhang, M. H. Chen, and Y. C. Wu, Cailiao Rechuli Xuebao/Transactions of Materials and Heat Treatment **41**, 7 (2020)
6. F. Liu, F. Lyu, F. Liu, X. Lin, and C. Huang, Journal of Materials Research and Technology **9**, 9753 (2020)
7. V. Santhosh, D. N. Agasia Prakash, K. Murugan, and N. Babu, Mater Today Proc **33**, 4445 (2020)
8. M. Liu, H. Fu, C. Xu, W. Xiao, Q. Peng, H. Yamagata, and C. Ma, Materials Science and Engineering: A **712**, 757 (2018)
9. J. K. Sunde, F. Lu, C. D. Marioara, B. Holmedal, and R. Holmestad, Materials Science and Engineering: A **807**, (2021)
10. Z. Gao, X. Zhang, H. Huang, C. Chen, J. Jiang, J. Niu, M. Dargusch, and G. Yuan, Mater Charact **185**, 111722 (2022)
11. A. B. Spierings, K. Dawson, P. J. Uggowitzer, and K. Wegener, Mater Des **140**, 134 (2018)
12. S. Thapliyal, M. Komarasamy, S. Shukla, L. Zhou, H. Hyer, S. Park, Y. Sohn, and R. S. Mishra, Materialia (Oxf) **9**, 100574 (2020)
13. M. M. Hoseini-Athar, R. Mahmudi, R. P. Babu, and P. Hedström, J Alloys Compd **831**, (2020)
14. J. Li, Z. Cao, L. Liu, X. Liu, and J. Peng, Steel Res Int **92**, 1 (2021)
15. M. Nazari, H. Eskandari, and F. Khodabakhshi, Surf Coat Technol **377**, 124914 (2019)
16. W. H. Liu, Z. P. Lu, J. Y. He, J. H. Luan, Z. J. Wang, B. Liu, Y. Liu, M. W. Chen, and C. T. Liu, Acta Mater **116**, 332 (2016)
17. Y. Bayat Asl, M. Meratian, A. Emamikhah, R. Mokhtari Homami, and A. Abbasi, Proc Inst Mech Eng B J Eng Manuf **229**, 1302 (2015)
18. H. C. Ananda Murthy and S. K. Singh, Adv Mater Lett **6**, 633 (2015)
19. S. Ma, Y. Zhao, J. Zou, K. Yan, and C. Liu, Opt Laser Technol **96**, 299 (2017)
20. D. H. Abdeen, M. El Hachach, M. Koc, and M. A. Atieh, Materials **12**, (2019)